ANL/NSE-21/25

SAS4A/SASSYS-1 Lead Verification Test Suite

Nuclear Science and Engineering Division

About Argonne National Laboratory

Argonne is a U.S. Department of Energy laboratory managed by UChicago Argonne, LLC under contract DE-AC02-06CH11357. The Laboratory's main facility is outside Chicago, at 9700 South Cass Avenue, Argonne, Illinois 60439. For information about Argonne and its pioneering science and technology programs, see www.anl.gov.

ANL/NSE-21/25

SAS4A/SASSYS-1 Lead Verification Test Suite

prepared by
D. O'Grady, A. Brunett, T. Sumner, L. Ibarra, T. Fanning, and R. Hu
Nuclear Science and Engineering Division, Argonne National Laboratory

June 2021

Abstract

SAS4A/SASSYS-1 is a simulation tool used to perform deterministic analyses of anticipated events as well as design basis and beyond design basis accidents for advanced liquid-metal-cooled nuclear reactors. With its origin as SAS1A in the late 1960s, the SAS series of codes has been under continuous use and development for over forty-five years and represents a critical investment in safety analysis capabilities for the U.S. Department of Energy. Although SAS4A/SASSYS-1 was developed to support the analysis of any liquid-metal-cooled nuclear reactor, it has primarily been utilized to design and analyze Sodium Fast Reactors (SFRs). As a result, most of the verification basis for SAS4A/SASSYS-1 utilizes sodium as a coolant and geometry descriptions that are typical of a SFR facility. In this work, new verification problems are defined to extend the applicability of the SAS4A/SASSYS-1 verification basis into Lead Fast Reactor (LFR) design space. A review of the existing SAS4A/SASSYS-1 SFR verification test suite is performed to determine the number of test cases that are SFR specific. SFR specific test cases are replicated using lead as a coolant and system layouts that are representative of LFRs. This report provides definitions and reference solutions for seven new test cases that scope lead-specific features and capabilities of the software. For a verification test to be considered acceptable, comparisons of analytical solutions to SAS4A/SASSYS-1 predictions must produce negligible or justifiable errors. All LFR specific test cases are found to be acceptable.

Table of Contents

1 Introduction

SAS4A/SASSYS-1 [1] is a simulation tool used to perform deterministic analysis of anticipated events as well as design basis and beyond design basis accidents for advanced liquid-metal-cooled nuclear reactors. With its origin as SAS1A in the late 1960s, the SAS series of codes has been under continuous use and development for over forty-five years and represents a critical investment in safety analysis capabilities for the U.S. Department of Energy. Although SAS4A/SASSYS-1 was developed to support the analysis of any liquid-metal-cooled nuclear reactor, it has primarily been utilized to design and analyze Sodium Fast Reactors (SFRs). As a result, most of the verification basis for SAS4A/SASSYS-1 utilizes sodium as a coolant and geometry descriptions that are typical of a SFR facility [2]. In this work, new verification problems are defined to extend the applicability of the SAS4A/SASSYS-1 verification basis into Lead Fast Reactor (LFR) design space.

New verification problems are defined in detail so that input decks can be prepared using only this document and the SAS4A/SASSYS-1 manual. Many of the test cases in this report include derivations of expected analytic solutions. As the verification cases become more complex, however, simple numerical models are used to provide reference solutions.

This report provides definitions and reference solutions that scope lead-specific features and capabilities of the software. For a test to be considered acceptable, comparisons of analytical solutions to SAS4A/SASSYS-1 predictions must be within defined acceptance criteria. Unacceptable tests, or those which do not pass, indicate a code deficiency which should be corrected.

Verification problems are designed to build incrementally with each test. This enables isolation of changes and testing of specific functionality or capabilities. The cases scoped in this report are listed in the table below. The first test case is utilized to establish a simple baseline test problem and is the case upon which the remaining cases are built.

The remaining sections of this report summarize the scope of the existing SAS4A/SASSYS-1 verification suite to LFRs and introduce new test cases to extend the extent of the code verification coverage. For each new test case, a description of the verification model will be provided along with the corresponding analytical solution. An acceptance criterion is defined for each of the verification models and a comparison of the SAS4A/SASSYS-1 against the analytical solution is presented.

2 SAS4A/SASSYS-1 V&V Test Suite

The SAS4A/SASSYS-1 V&V Test Suite currently contains over 300 test cases. These tests incorporate verification, validation and training input models for various components and system configuration. Reference [2] provides an overview of the verification and validation cases available, while [3] describes in further detail the validation effort for the SAS4A/SASSYS-1 RVACS component model. A summary of the verification test cases is provided in Table 2-1.

Table 2-1 Overview of the SAS4A/SASSYS-1 Verification Test Suite

Case	Description
	Simple Steady State Cases
1.1	Base test case
1.1.x	Mesh refinement study
1.2	Increasing the number of pins
1.3	Increasing the number of assemblies
1.4	Increasing the number of core channels
1.5	Adding 3 lower reflectors and 3 upper reflectors with an upper fission gas plenum
1.6	Adding 3 lower reflectors and 3 upper reflectors with a lower fission gas plenum
1.6.x	Mesh refinement study
1.7	Adding 1 lower reflector and 5 upper reflectors
1.8	Adding 5 lower reflectors and 1 upper reflector
1.9	Form loss pressure drop in the channel
	Simple Transient Cases
2.1	Maintaining steady state temperatures during the transient
2.2	Increasing reactor power
2.2.x	Mesh refinement study
2.3	Increasing core inlet temperature
2.4	Decreasing sodium mass flow rate
	Material Properties Cases
3.1	Using the temperature-dependent sodium density
3.2	Using the temperature-dependent sodium heat capacity
3.3	Using the temperature-dependent sodium thermal conductivity and convective heat transfer coefficient

3.4	Using the temperature-dependent cladding thermal conductivity
3.5	Using the temperature-dependent fuel thermal conductivity
3.5.x	Mesh refinement study
3.6	Using the temperature-dependent built-in sodium properties
3.7	Using the 15-15 Ti Cladding properties
	Core Power Cases
4.1	Sinusoidal power axial profile
4.2	Point kinetics vs. user-defined total power
4.3	Old decay heat model with one group
4.4	Old decay heat model with six groups
4.5	New decay heat model with six groups
4.6	ANS decay heat standard using new decay heat model
4.7	ANS decay heat standard model
4.7.x	Mesh refinement study
4.8	Combination of new decay heat model and ANS decay heat standard model
4.9	External reactivity insertion at zero power
4.10	External reactivity insertion at full power
4.11	Doppler reactivity feedback
4.11.x	Mesh refinement study
4.12	Axial fuel expansion reactivity feedback
4.12.x	Mesh refinement study
4.13	Axial cladding expansion reactivity feedback
4.14	Axial fuel and cladding expansion reactivity feedback, independent expansion option
4.15	Axial fuel and cladding expansion reactivity feedback, clad-based option
4.16	Axial fuel and cladding expansion reactivity feedback, force balance option
4.17	Axial structure expansion reactivity feedback
4.18	Sodium void reactivity feedback
4.18.x	Mesh refinement study
4.19	Modeling feedbacks on the MZ and MZC meshes

4.19.x	Mesh refinement study
4.20	Control rod driveline expansion reactivity feedback
4.21	Vessel expansion reactivity feedback
4.22	Radial core expansion reactivity feedback
	Heat Removal Systems Cases
5.1	Steady state PRIMAR-4 temperatures
5.2	Maintaining PRIMAR-4 temperatures during the transient
5.3	User-defined temperature drop simple IHX model
5.4	User-defined outlet temperature simple IHX model
5.5	Detailed IHX model
5.6	Introducing a second heat exchanger
5.7	Friction pressure drop
5.7.x	Mesh refinement study
5.8	Bends pressure drop
5.9	Form loss pressure drop
5.10	Gravity pressure drop
5.11	Acceleration pressure drop
5.12	Steady state pump head
5.13	Valve loss coefficient
5.14	User-defined temperature drop simple steam generator model
5.15	User-defined outlet temperature simple steam generator model
5.16	Equilibrating to and maintaining new temperatures in a transient
5.17	Heat transfer between an element and a constant temperature external heat source
5.18	Heat transfer between a compressible volume and a constant temperature external heat source
5.19	Natural circulation without orifice coefficients or bends
5.20	Natural circulation with form loss pressure drops
5.21	Natural circulation with bends pressure drops
5.22	Core reference elevation
5.22.x	Mesh refinement study
5.23	Heat transfer between an element and a simple RVACS
5.24	Heat transfer between a compressible volume and a simple RVACS

5.25	Heat transfer between an element and a coupled RVACS
5.26	Heat transfer between a thick-walled compressible volume and a constant temperature external heat source
5.27	Detail Primary Heat Exchanger
	Control Systems Cases
6.1	Block signals (simple mathematical and logic), demand table signals, time signal
6.2	Dynamic block signals
6.3	HTS temperature and density measured signals
6.4	HTS pressure and flow measured signals

Verification test cases are developed using the methodology presented in [2]. Analytic solutions have been derived in [4-9] and comparisons have been made between the SAS4A/SASSYS-1 predictions and the analytical solutions in [4-9]. All verification cases presented in Table 2-1 meet their respective acceptance criterion. Mesh refinement studies have been performed for several verification cases in order to determine the limiting mesh size that satisfies the corresponding acceptance criterion [10].

The majority of the verification cases utilize sodium as the reactor coolant and are based on facility layouts that are characteristic of an SFR. At a more granular level, many of the verification test cases can be considered coolant agnostic. These test cases include:

- Cases 1.2 - Case 1.9, which verify that SAS4A/SASSYS-1 correctly captures additional complexity that can be built on top of a base model.
- Case 2.1 - Case 2.4, which verify that the transient solver routines correctly predict the base model response to a zero transient, or simple change in the boundary conditions.
- Case 4.1 - Case 4.22, which verify the core power models.
- Case 5.17, Case 5.18, and Case 5.23 – Case 5.26, which verify that SAS4A/SASSYS-1 correctly captures heat transfer between components.
- Case 6.1 – Case 6.4, which verify the control system logic and its ability to read measured signals.

In order to extend the coverage of the SAS4A/SASSYS-1 verification test suite into LFR design space, several of the SFR specific test cases need to be recreated for lead as a coolant and facility layouts that are more representative of an LFR. In order to reduce the number of new test cases that need to be created, the SFR specific test cases were further analyzed to identify overlapping characteristics. Case 1.10 is a recreation of Case 1.1 using channel dimensions that are representative of an LFR to provide a base case for LFR testing. Cases 3.8 – 3.11 are recreations of Cases 3.1 – 3.6, respectively, to confirm that the built-in lead coolant thermophysical properties are utilized correctly. The mesh refinement study, performed on Case 3.5 for sodium coolant, will not be duplicated. Mesh refinement studies are left to the end user, who will need

to perform spatial discretization studies for their specific design and plant configuration. Cases 5.1, 5.16, and 5.27 will be combined as Case 5.28 in order to demonstrate that SAS4A/SASSYS-1 correctly distributes the steady state coolant temperatures, and transitions to a new equilibrium temperature distribution using a primary heat exchanger for an LFR facility layout. Cases 5.7 – 5.12 and Cases 5.19 – 5.21 will be combined as Case 5.29 in order to demonstrate that SAS4A/SASSYS-1 correctly distributes and maintains the pressure throughout the primary system for an LFR facility layout. Collectively, these test cases capture all of the SFR specific verification testing that has been performed and extend the coverage into LFR design space. A summary of the new test cases is presented in Table 2-2.

Table 2-2 Overview of new SAS4A/SASSYS-1 LFR-based Verification Test Cases

Case	Description
	Simple Steady State Cases
1.10	Base LFR Fuel Channel
	Material Property Cases
3.8	LFR Temperature-Dependent Coolant Density
3.9	LFR Temperature-Dependent Coolant Heat Capacity
3.10	LFR Temperature-Dependent Coolant Thermal Conductivity
3.11	Temperature-Dependent Built-In Lead Properties
	Heat Removal System Cases
5.28	LFR Equilibrium Temperature Distribution
5.29	LFR Equilibrium Pressure Distribution

3 Simple Steady State Cases

The first case is the LFR fuel channel test case from which all other LFR tests are derived.

3.1 LFR Fuel Channel Test Case

3.1.1 Test Description

The LFR Fuel Channel test case is a steady state test problem for a single pin with uniform dimensions and constant properties, bounded at the top and bottom of the fuel pin. The fuel pin has a constant linear heat generate rate of 14.23 kW/m. Lead coolant enters from the bottom at 0.98 kg/s and a temperature of 693.15 K. The exit pressure at the top of the pin is 0.661 MPa. No hex can is defined. All necessary dimensions and properties of the fuel, cladding, and coolant are given in Table 3-1. The parameters are considered representative of a lead cool reactor system.

Table 3-1 Parameters of the LFR Fuel Channel Case

General		
# Pins	-	1
Coolant Inlet Temp	K	693.15
Mass Flow Rate Per Pin	kg/s	0.98
Total Power	W	15000
Pin Dimensions		
Fuel Height	m	1.05
Fuel Radius	m	4.275E-03
Cladding Inner Radius	m	4.450E-03
Cladding Outer Radius	m	5.350E-03
Hydraulic Diameter	m	8.044E-03
Coolant Flow Area	m^2	6.760E-05
Wetted Perimeter	m	3.362E-02
Thermo-Physical Properties		
Fuel Thermal Conductivity	W/m-K	2.8
Cladding Thermal Conductivity	W/m-K	23.8
Gap Thermal Conductivity	W/m-K	0.289
Coolant Density	kg/m^3	11441
Coolant Heat Capacity	J/kg-K	245
Coolant Thermal Conductivity	W/m-K	9.2
Coolant Heat Transfer Coefficient	W/m^2-K	8.0E+03
Coolant Viscosity	Pa-s	3.48E-04
Other Values		
Friction Factor		0.013134
Pressure at Core Outlet	Pa	6.61E+05

Material properties and thermal hydraulic parameters such as the friction factor and convective heat transfer coefficient are held constant.

3.1.2 Acceptance Criteria

The test case is considered acceptable if there is agreement between SAS4A/SASSYS-1 results and the analytical solution for the following Quantities of Interest (QOI):

- Fuel centerline temperature,
- Fuel surface temperature,
- Cladding inner surface temperature,
- Cladding outer surface temperature,
- Coolant temperature, and
- Axial pressure distribution with the coolant channel.

All temperature QOIs must be within 0.1 K of the analytic solution. All pressure QOIs must be within 0.1 kPa. These values were selected based on the minimum precision of the standard output.

3.1.3 Analytical Solution

At the fuel pin level, the primary variable of interest is the temperature distribution. Chapter 13 of [11] provides an analytical solution for axial temperature profiles in the case of sinusoidal axial power generation. A similar method is used in the solutions below using a uniform axial power profile.

3.1.3.1 Bulk Coolant

Equation (3-1) presents a reduced form of the energy equation in a coolant channel at steady state with constant flow area. The terms for pressure gradient and friction dissipation are neglected:

$$\dot{m}\frac{d}{dz}\,h_{Pb} = q'(z) \tag{3-1}$$

where $\dot{m}$ is mass flow rate of coolant, h_{Pb} is specific enthalpy of the lead coolant, and $q'(z)$ is the linear heat generation rate. For a constant linear heat generation rate, $q'(z) = q'$, and a constant specific heat capacity, c_p, integrating Equation (3-1) over the axial length gives:

$$T_c(z) = T_{\text{in}} + \frac{q'\cdot z}{\dot{m}\,c_p} \tag{3-2}$$

where, $T_c(\text{z})$ is the axial coolant temperature and $T_c(0)$ equals T_{in}.

3.1.3.2 Cladding Outer Surface Temperature

The axial temperature profile at the outer cladding surface can be found using Newton's Law of Cooling:

$$q''(z)A = \text{h}_\text{c}\,A\,\Delta T \tag{3-3}$$

This can be rearranged to give:

$$q'(z) = 2\pi R_{co} \mathrm{h_c} \left(T_{co}(z) - T_c(z)\right) \tag{3-4}$$

where R_{co} is the radius of the outer cladding surface, T_{co} is the radius of the outer cladding surface and h_c is the convective heat transfer coefficient. By assuming a constant linear heat generation rate, $q'(z) = q'$, the cladding outer surface temperature can be determined using Equation (3-4):

$$T_{co}(z) = T_c(z) + \frac{\mathrm{q'}}{2\,\pi\,\mathrm{R_{co}}\,h_c} \tag{3-5}$$

3.1.3.3 Cladding Inner Surface Temperature

By assuming that axial conduction can be neglected, the temperature at the cladding inner surface can be found starting with the steady state heat conduction equation in cylindrical coordinates:

$$\frac{1}{\mathrm{r}}\frac{d}{dr}\left(k_{clad} r \frac{dT}{dr}\right) + q''' = 0 \tag{3-6}$$

By assuming gamma heating is negligible, i.e., the volumetric heat generation in the cladding is zero, integrating once produces:

$$k_{clad}\frac{dT}{dr} = \frac{C_1}{r} \tag{3-7}$$

where C_1 is a constant. Noting that at the inner cladding surface, R_{ci}, conservation of energy requires $-k_{clad}\frac{dT}{dr} = q'' = \frac{q'}{2\pi R_{ci}}$, therefore C_1 equals $-\frac{q'}{2\pi}$. By integrating the previous equation from the cladding outer surface to the clad inner surface produces:

$$k_{clad}\left(T_{co}(z) - T_{ci}(z)\right) = -\frac{q'}{2\pi}\ln\left(\frac{R_{co}}{R_{ci}}\right) \tag{3-8}$$

where $T_{ci}(z)$ is the axial temperature distributions at the inner cladding surface. Solving Equation (3-8) for $T_{ci}(z)$ gives:

$$T_{ci}(z) = T_{co}(z) + \frac{q'}{2\pi k_{clad}}\ln\left(\frac{r_{co}}{r_{ci}}\right) \tag{3-9}$$

3.1.3.4 Fuel Outer Surface Temperature

The fuel surface temperature, $T_{fs}(z)$ can be found using an equation similar to Equation (3-5) for the cladding outer surface temperature:

$$h_g \left(T_{fs}(z) - T_{ci}(z)\right) = \frac{q'}{2\,\pi\,R_f} \tag{3-10}$$

where $h_g = \frac{k_g}{\tau_g}$ is the heat transfer coefficient of the gap, defined as the thermal conductivity of the gap, k_g, divided by the gap thickness, τ_g, and R_f is the radius at the fuel outer surface. Fuel surface temperature is:

$$T_{fs}(z) = T_{\mathrm{ci}}(z) + \frac{q'}{2\,\pi\,R_f\,h_g} \tag{3-11}$$

3.1.3.5 Fuel Centerline Temperature

For the cylindrical fuel region, the steady state heat conduction equation with volumetric heat generation q''' is:

$$\frac{1}{r}\frac{d}{dr}\left(kr\frac{dT}{dr}\right) + q''' = 0 \tag{3-12}$$

Assuming q''' is constant, integrating the previous equation gives:

$$k\frac{dT}{dr} + q'''\frac{r}{2} + \frac{C_1}{r} = 0 \tag{3-13}$$

For solid fuel at the center of the pin, $r = 0$, the fuel temperature must be finite, therefore Equation (3-13) simplifies to:

$$k\frac{dT}{dr} + q'''\frac{r}{2} = 0 \tag{3-14}$$

By assuming a uniform volumetric heat generation, $q''' = \frac{q'}{\pi R_{fo}^2}$, and a temperature independent thermal conductivity, k_f, integrating the previous equation from the fuel surface to some radius, r, gives:

$$T_f(r,z) = \mathrm{T_{fs}(z)} + \frac{q'\left(R_{fo}^2 - r^2\right)}{4\pi R_{fo}^2 k_f} \tag{3-15}$$

The fuel centerline temperature is:

$$T_{CL}(z) = T_f(0,z) = T_{fs}(z) + \frac{q'}{4\,\pi\,k_f} \tag{3-16}$$

All of the parameters needed to calculate the analytical axial and radial temperature profiles are given in Table 3-1. Because all material properties are temperature-independent, the shape of the radial temperature profile is constant at all axial locations. The resulting axial temperature profiles are illustrated in Figure 3.3-1. Table 3-2 provides the axial temperature profile results in 5.25 cm intervals. The radial fuel temperature profile, presented in Table 3-3, was generated using 9 nodes of equal width.

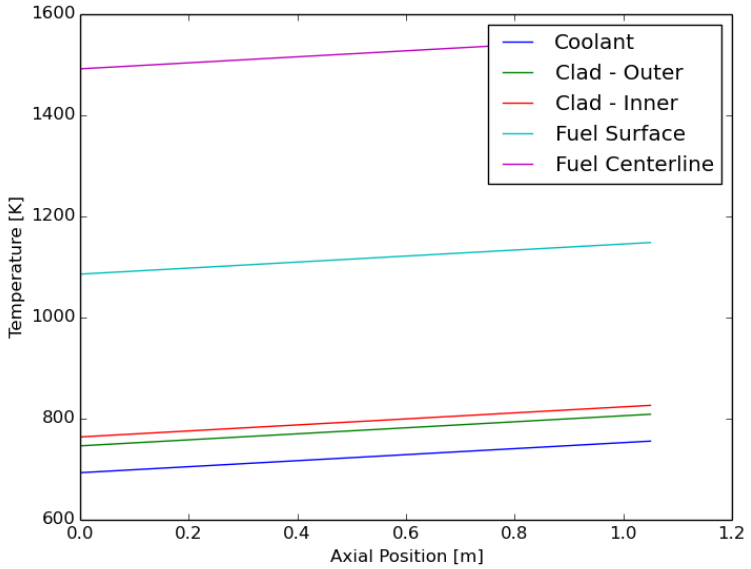

Figure 3.3-1. Baseline Test Case: Analytical Temperature Solution

Table 3-2 LFR Fuel Channel Case: Analytical Temperature Solution (K)

Axial Position (m)	Avg. Coolant	Clad Outer	Clad Inner	Fuel Surface	Fuel Centerline
1.024	754.062	807.185	824.781	1146.833	1552.840
0.971	750.938	804.061	821.657	1143.709	1549.717
0.919	747.815	800.937	818.533	1140.585	1546.593
0.866	744.691	797.814	815.410	1137.462	1543.469
0.814	741.567	794.690	812.286	1134.338	1540.346
0.761	738.444	791.566	809.162	1131.214	1537.222
0.709	735.320	788.442	806.039	1128.091	1534.098
0.656	732.196	785.319	802.915	1124.967	1530.974
0.604	729.073	782.195	799.791	1121.843	1527.851
0.551	725.949	779.071	796.667	1118.720	1524.727
0.499	722.825	775.948	793.544	1115.596	1521.603
0.446	719.701	772.824	790.420	1112.472	1518.480
0.394	716.578	769.700	787.296	1109.348	1515.356
0.341	713.454	766.577	784.173	1106.225	1512.232
0.289	710.330	763.453	781.049	1103.101	1509.109
0.236	707.207	760.329	777.925	1099.977	1505.985
0.184	704.083	757.205	774.802	1096.854	1502.861
0.131	700.959	754.082	771.678	1093.730	1499.737
0.079	697.836	750.958	768.554	1090.606	1496.614
0.026	694.712	747.834	765.430	1087.483	1493.490

Table 3-3 LFR Fuel Channel Case: Analytical Radial Fuel Temperatures Distribution (K)

Axial Position (m)	Radial Fuel Position (cm)								
	0.0000	0.0534	0.1069	0.1603	0.2138	0.2672	0.3206	0.3741	0.4275
1.024	1552.8	1546.5	1527.5	1495.8	1451.3	1394.2	1324.5	1241.9	1146.8
0.971	1549.7	1543.4	1524.3	1492.6	1448.2	1391.1	1321.4	1238.8	1143.7
0.919	1546.6	1540.3	1521.2	1489.5	1445.0	1388.0	1318.2	1235.7	1140.6
0.866	1543.5	1537.1	1518.1	1486.4	1441.9	1384.9	1315.1	1232.6	1137.5
0.814	1540.3	1534.0	1515.0	1483.3	1438.8	1381.7	1312.0	1229.4	1134.3
0.761	1537.2	1530.9	1511.8	1480.1	1435.7	1378.6	1308.9	1226.3	1131.2
0.709	1534.1	1527.8	1508.7	1477.0	1432.5	1375.5	1305.8	1223.2	1128.1
0.656	1531.0	1524.6	1505.6	1473.9	1429.4	1372.4	1302.6	1220.1	1125.0
0.604	1527.9	1521.5	1502.5	1470.8	1426.3	1369.2	1299.5	1216.9	1121.8
0.551	1524.7	1518.4	1499.3	1467.6	1423.2	1366.1	1296.4	1213.8	1118.7
0.499	1521.6	1515.3	1496.2	1464.5	1420.1	1363.0	1293.3	1210.7	1115.6
0.446	1518.5	1512.1	1493.1	1461.4	1416.9	1359.9	1290.1	1207.6	1112.5
0.394	1515.4	1509.0	1490.0	1458.3	1413.8	1356.7	1287.0	1204.4	1109.3
0.341	1512.2	1505.9	1486.8	1455.1	1410.7	1353.6	1283.9	1201.3	1106.2
0.289	1509.1	1502.8	1483.7	1452.0	1407.6	1350.5	1280.8	1198.2	1103.1
0.236	1506.0	1499.6	1480.6	1448.9	1404.4	1347.4	1277.6	1195.1	1100.0
0.184	1502.9	1496.5	1477.5	1445.8	1401.3	1344.2	1274.5	1191.9	1096.9
0.131	1499.7	1493.4	1474.4	1442.7	1398.2	1341.1	1271.4	1188.8	1093.7
0.079	1496.6	1490.3	1471.2	1439.5	1395.1	1338.0	1268.3	1185.7	1090.6
0.026	1493.5	1487.2	1468.1	1436.4	1391.9	1334.9	1265.1	1182.6	1087.5

3.1.3.6 Coolant Pressure

The analytical solution for coolant pressure has two components: gravity pressure drop and friction pressure drop. For a channel with constant coolant density and consistent flow area, there is no acceleration pressure drop. The pressure drop due to gravity from the coolant outlet to axial position z is:

$$\Delta p_{\text{grav}}(z) = \int \rho_c \cdot g \cdot dz = \rho_c \cdot g \cdot (z_{\text{outlet}} - z) \tag{3-17}$$

The pressure drop due to friction is found using the following equation:

$$\Delta p_{\text{fric}}(z) = \int \frac{f\,\dot{m}^2}{2 \cdot \rho_c \cdot D_h \cdot A^2}\, dz = \frac{f\,\dot{m}^2}{2 \cdot \rho_c \cdot D_h \cdot A^2}\,(z_{\text{outlet}} - z) \tag{3-18}$$

Combining these two equations with the coolant outlet pressure, P_{outlet}, gives a pressure distribution of:

$$p(z) = p_{\text{outlet}} + \left[\rho_c \cdot g + \frac{f\,\dot{m}^2}{2 \cdot \rho_c \cdot D_h \cdot A^2}\right] \cdot (z_{\text{outlet}} - z) \tag{3-19}$$

Because SAS4A/SASSYS-1 assumes a value of 9.7805 $\frac{m}{s^2}$ for acceleration due to gravity, this value was used in the analytical solution. Table 3-4 provides the gravitational and frictional pressure drop values, as measured from the outlet, alongside the coolant pressure in 5.25 cm increments.

Table 3-4 LFR Fuel Channel Case: Analytical Pressure Solution (Pa)

Axial Position (m)	Gravity ΔP	Friction ΔP	Coolant Pressure
1.0500	0	0	661000
0.9975	5875	787	667662
0.9450	11749	1575	674324
0.8925	17624	2362	680986
0.8400	23499	3149	687648
0.7875	29373	3937	694310
0.7350	35248	4724	700972
0.6825	41123	5511	707634
0.6300	46997	6299	714296
0.5775	52872	7086	720958
0.5250	58747	7873	727620
0.4725	64621	8660	734282
0.4200	70496	9448	740944
0.3675	76371	10235	747606
0.3150	82246	11022	754268
0.2625	88120	11810	760930
0.2100	93995	12597	767592
0.1575	99870	13384	774254
0.1050	105744	14172	780916
0.0525	111619	14959	787578
0.0000	117494	15746	794240

3.1.4 Results Summary

All QOIs are within their respective acceptance criteria. A simplification in the cladding inner surface temperature solution results in an error propagation into the fuel radial temperature. A summary of the results is provided in Table 3-5.

Table 3-5 Summary of Results for LFR Fuel Channel Case

QOI	Result	Notes
Coolant Temperature	Pass	
Cladding Outer Surface Temperature	Pass	
Cladding Inner Surface Temperature	Pass	
Fuel Radial Temperatures	Pass	
Gravity Pressure Drop	Pass	
Frictional Pressure Drop	Pass	
Total Pressure Drop	Pass	

3.1.4.1 Temperature Results

The LFR fuel channel case utilizes several constant properties and coefficients. Lead specific heat, density, and thermal conductivity were defined using the PMATCM: APROPI input to override the built-in lead correlations. The lead heat transfer coefficient was fixed by setting c_1 and c_2 to zero in the following equation

$$h = \frac{k}{D_h} \times \left(c_1 \left[\frac{D_h \, \dot{m} \, c_p}{k \, A_c} \right]^{c_2} + c_3 \right) \tag{3-20}$$

With a lead thermal conductivity of 23.8 $W/m-K$ and a hydraulic diameter of 8.044E-03 m, setting c_3 to 6.9945 produces the desired heat transfer coefficient of 8E3 W/m^2-K.

For turbulent flow, SAS calculates the friction factor as

$$f = A_{fr} \times Re^{b_{fr}} \tag{3-21}$$

To fix the friction factor at 0.013134, A_{fr} and b_{fr} were set to 0.013134 and 1.0E-09, respectively. In order to separate the frictional pressure drop from the gravitational pressure drop, a second core channel was introduced with identical dimensions as the first channel. In the second core channel, the friction factor was set to effectively zero by setting A_{fr} and b_{fr} to 1.0E-06 and -1.0E+06, respectively. The frictional pressure drop contribution can be calculated using the difference of the channel 1 coolant pressure, which accounts for friction and gravity, and channel 2 coolant pressure, which only accounts for gravity.

A SAS4A/SASSYS-1 model of the LFR channel case produced the fuel, cladding, and coolant temperatures. The differences between the SAS4A/SASSYS-1 predictions and the analytical values are listed in Table 3-6 and Table 3-7.

The small difference in the cladding temperatures is caused by SAS4A/SASSYS-1 assuming that the cladding is very thin. This allows for the approximation of linear temperature increases from the cladding outer surface to cladding midpoint and from cladding midpoint to cladding inner surface. The difference from this approximation is very small and is considered acceptable.

Table 3-6 LFR Fuel Channel Case: Axial Temperature Errors (K)

Axial Position (m)	Avg. Coolant	Clad Outer	Clad Inner	Fuel Surface	Fuel Centerline
1.024	0.000	-0.000	0.013	0.013	0.012
0.971	0.000	-0.000	0.012	0.012	0.013
0.919	-0.000	0.000	0.012	0.012	0.013
0.866	0.000	-0.000	0.013	0.013	0.012
0.814	0.000	-0.000	0.013	0.012	0.013
0.761	-0.000	0.000	0.012	0.012	0.013
0.709	-0.000	0.000	0.013	0.013	0.012
0.656	0.000	-0.000	0.013	0.013	0.012
0.604	-0.000	0.000	0.012	0.012	0.013
0.551	-0.000	0.000	0.012	0.013	0.012
0.499	0.000	-0.000	0.013	0.013	0.012
0.446	0.000	-0.000	0.012	0.012	0.013
0.394	-0.000	0.000	0.012	0.012	0.013
0.341	0.000	-0.000	0.013	0.013	0.012
0.289	0.000	-0.000	0.013	0.012	0.013
0.236	-0.000	0.000	0.012	0.012	0.013
0.184	-0.000	0.000	0.013	0.013	0.012
0.131	0.000	-0.000	0.013	0.013	0.012
0.079	-0.000	0.000	0.012	0.012	0.013
0.026	-0.000	0.000	0.012	0.013	0.012

Table 3-7 LFR Fuel Channel Case: Radial Temperature Errors (K)

Axial Position (m)	Radial Fuel Position (cm)								
	0.0000	0.0534	0.1069	0.1603	0.2138	0.2672	0.3206	0.3741	0.4275
1.024	0.012	0.021	0.001	0.021	-0.035	-0.002	0.048	-0.049	0.013
0.971	0.013	0.022	0.000	0.022	-0.035	-0.002	0.048	-0.050	0.012
0.919	0.013	0.021	0.001	0.021	-0.035	-0.003	0.048	-0.050	0.012
0.866	0.012	0.021	0.001	0.021	-0.035	-0.002	0.048	-0.050	0.013
0.814	0.013	0.022	0.000	0.022	-0.035	-0.002	0.048	-0.050	0.012
0.761	0.013	0.022	0.001	0.021	-0.035	-0.003	0.048	-0.050	0.012
0.709	0.012	0.021	0.001	0.021	-0.035	-0.002	0.049	-0.050	0.013
0.656	0.012	0.022	0.001	0.022	-0.035	-0.002	0.048	-0.049	0.013
0.604	0.013	0.022	0.000	0.022	-0.035	-0.003	0.048	-0.050	0.012
0.551	0.012	0.021	0.001	0.021	-0.035	-0.002	0.048	-0.050	0.013
0.499	0.012	0.021	0.001	0.021	-0.035	-0.002	0.048	-0.049	0.013
0.446	0.013	0.022	0.000	0.022	-0.035	-0.002	0.048	-0.050	0.012
0.394	0.013	0.021	0.001	0.021	-0.035	-0.003	0.048	-0.050	0.012
0.341	0.012	0.021	0.001	0.021	-0.035	-0.002	0.048	-0.050	0.013
0.289	0.013	0.022	0.000	0.022	-0.035	-0.002	0.048	-0.050	0.012
0.236	0.013	0.021	0.001	0.021	-0.035	-0.003	0.048	-0.050	0.012
0.184	0.012	0.021	0.001	0.021	-0.035	-0.002	0.049	-0.050	0.013
0.131	0.012	0.022	0.000	0.022	-0.035	-0.002	0.048	-0.049	0.013
0.079	0.013	0.022	0.000	0.022	-0.035	-0.003	0.048	-0.050	0.012
0.026	0.012	0.021	0.001	0.021	-0.035	-0.002	0.048	-0.050	0.013

3.1.4.2 Pressure Results

The SAS4A/SASSYS-1 model used to predict LFR fuel channel case temperatures was also used to predict the axial pressure distribution. The difference between the simulation and the analytical solution pressures are listed in Table 3-8. SAS4A/SASSYS-1 reports pressures in the output file in MPa and any differences between the solutions are less than the accuracy of the printed values. The SAS4A/SASSYS-1 axial pressure distributions agree very well with the analytical solution for the LFR fuel channel case.

Table 3-8 LFR Fuel Channel Case: Pressure Errors (MPa)

Axial Position (m)	Gravity ΔP	Friction ΔP	Coolant Pressure
1.0500	0.0000	0.0000	0.0000
0.9975	0.0000	-0.0000	-0.0000
0.9450	-0.0000	-0.0000	-0.0000
0.8925	-0.0000	0.0001	0.0000
0.8400	0.0000	-0.0001	-0.0000
0.7875	0.0000	0.0000	0.0000
0.7350	-0.0000	0.0000	0.0000
0.6825	-0.0000	0.0000	-0.0000
0.6300	0.0000	-0.0000	0.0000
0.5775	0.0000	-0.0000	-0.0000
0.5250	-0.0000	0.0001	0.0000
0.4725	-0.0000	0.0001	0.0000
0.4200	0.0000	-0.0001	-0.0000
0.3675	0.0000	0.0000	0.0000
0.3150	-0.0000	0.0000	-0.0000
0.2625	-0.0000	0.0000	-0.0000
0.2100	0.0000	-0.0000	0.0000
0.1575	-0.0000	-0.0000	-0.0000
0.1050	-0.0000	0.0001	0.0000
0.0525	0.0000	-0.0000	0.0000
0.0000	0.0000	-0.0001	-0.0000

4 Temperature Dependent Material Property Cases

This group of test cases introduces temperature-dependent coolant material properties that affect steady state temperatures. The geometry defined for the LFR fuel channel test case is assumed for each case. Because only steady state analytical solutions have been generated, tests for properties that would affect only the transient results, e.g. fuel heat capacity, have not been included. Each material property change is maintained for subsequent cases until the final case in this section.

4.1 Coolant Density

4.1.1 Test Description

For this test the coolant density is updated from a constant value to a linear temperature dependency:

$$\rho_c(T) = 1.144 \times 10^4 - 1.28T \tag{4-1}$$

where temperature is in Kelvin. This change affects the gravity and friction pressure drops and introduces an acceleration pressure drop.

4.1.2 Acceptance Criteria

The test case is considered acceptable if there is reasonable agreement between SAS4A/SASSYS-1 results and the analytical solution for the following QOI:

- Pressure difference between the inlet and outlet of the coolant channel.

All pressure QOIs must be within 0.1 kPa.

4.1.3 Analytical Solution

4.1.3.1 Gravitational Pressure Drop

The gravity pressure drop between z_1 and z_2 is given by

$$\begin{aligned} \Delta p_{\text{grav}}(z_{1,2}) &= \int_{z_1}^{z_2} \rho_c\big(T_c(z)\big) \cdot g \cdot dz \\ &= \int_{z_1}^{z_2} \big(1.144 \times 10^4 - 1.28 T_c(z)\big) \cdot g \cdot dz \end{aligned} \tag{4-2}$$

In the core region, $T_c(z)$ is given by Equation (3-2). Substitution into the previous equation gives:

$$\Delta p_{\text{grav}}(z_{1,2}) = \int_{z_1}^{z_2} \left(1.144 \times 10^4 - 1.28\left(T_{\text{in}} + \frac{q' \cdot z}{\dot{m}\, c_p}\right)\right) \cdot g \cdot dz \tag{4-3}$$

which reduces to:

$$\Delta p_{\text{grav}}(z_{1,2}) = (1.144 \times 10^4 - 1.28 T_{\text{in}}) g\ (z_2 - z_1) - \frac{1.28 \cdot q' \cdot g}{2\ \dot{m}\ c_p}\ (z_2^2 - z_1^2) \tag{4-4}$$

4.1.3.2 Friction Pressure Drop

Combining Equations (3-18) and (4-1) for the friction pressure drop gives:

$$\Delta p_{\text{fric}}(z_{1,2}) = \int_{z_1}^{z_2} \frac{f\ \dot{m}^2}{2\ \rho_c(T_c(z)) D_h\ A^2}\ dz = \int_{z_1}^{z_2} \frac{f\ \dot{m}^2}{2 \cdot \left(1.144 \times 10^4 - 1.28 T_c(z)\right) \cdot D_h \cdot A^2}\ dz \tag{4-5}$$

Substituting the coolant temperature profile into the previous equation gives:

$$\Delta p_{\text{fric}}(z_{1,2}) = \frac{f\ \dot{m}^2}{2 \cdot D_h \cdot A^2} \int_{z_1}^{z_2} \frac{1}{1.144 \times 10^4 - 1.28\left(T_{\text{in}} + \frac{q' \cdot z}{\dot{m}\ c_p}\right)} dz \tag{4-6}$$

This simplifies to:

$$\Delta p_{\text{fric}}(z_{1,2}) = \frac{f\ \dot{m}^2}{2 \cdot D_h \cdot A^2} \frac{\ln(C_1 - C_2\ z_1) - \ln(C_1 - C_2\ z_2)}{C_2} \tag{4-7}$$

where $C_1 = 1.144 \times 10^4 - 1.28 T_{\text{in}}$, and $C_2 = \frac{1.28\ q'}{\dot{m}\ c_p}$.

4.1.3.3 Acceleration Pressure Drop

Because the coolant density now varies axially, a small pressure drop due to acceleration is introduced. This pressure drop is defined as:

$$\Delta p_{\text{acc.}}(z_{1,2}) = \frac{\dot{m}^2}{A^2} \left(\frac{1}{\rho(T_c(z_2))} - \frac{1}{\rho(T_c(z_1))} \right) \tag{4-8}$$

Combining the previous equation with Equations (4-1) and (3-2) gives:

$$\Delta p_{\text{acc.}}(z_{1,2}) = \frac{\dot{m}^2}{A^2}\left(\frac{1}{1.144\times 10^4 - 1.28\left(T_{\text{in}} + \frac{q'\cdot z_2}{\dot{m}\, c_p}\right)} - \frac{1}{1.144\times 10^4 - 1.28\left(T_{\text{in}} + \frac{q'\cdot z_1}{\dot{m}\, c_p}\right)}\right) \tag{4-9}$$

4.1.3.4 Coolant Pressure

The axial coolant pressure can be found by summing up the drop contributions in each coolant node.

$$p(z_{in}) = p(z_{out}) + \Delta p_{\text{acc.}}(z_{in,out}) + \Delta p_{fric}(z_{in,out}) + \Delta p_{\text{grav}}(z_{in,out}) \tag{4-10}$$

By assuming 9.7805 $\frac{m}{s^2}$ for acceleration due to gravity, the pressure difference from the inlet to the outlet of the core channel can be determined. Table 4-1 contains the total pressure drop from the inlet to the outlet as well as the contribution from gravity, acceleration and friction.

Table 4-1 Variable Density Analytical Pressure Drop (Pa)

Component	Pressure Drop (Pa)
Gravity	107961.3
Friction	17136.7
Acceleration	152.1
Total	125250.0

4.1.4 Results Summary

All QOIs are within their respective acceptance criteria. The difference between the simulation and the analytical solution pressures is 50 Pa. The difference between the solutions is less than the printed output data accuracy. The SAS4A/SASSYS-1 pressure drop agrees very well with the analytical solution for the LFR fuel channel case with temperature dependent density.

4.2 Coolant Heat Capacity

4.2.1 Test Description

For this case, the heat capacity of the coolant is updated from a constant value to:

$$c_p(T) = 150 - 0.01\,T \tag{4-11}$$

where the temperature is in Kelvin and c_p is in $\frac{J}{kg-K}$.

4.2.2 Acceptance Criteria

The test case is considered acceptable if there is reasonable agreement between SAS4A/SASSYS-1 results and the analytical solution for the following QOI:

- Fuel centerline temperature,
- Fuel surface temperature,
- Cladding inner surface temperature,
- Cladding outer surface temperature,
- Coolant temperature.

All temperature QOIs must be within 0.1 K of the analytic solution.

4.2.3 Analytic Solution

For single-phase coolant with temperature-independent properties, Equation (3-2) gives the axial coolant temperature profile for a constant linear heat generation rate, $q'(z) = q'$. However, because heat capacity is temperature-dependent for this case, the heat capacity term must remain inside the integral in:

$$\dot{m} \int_{T_{\text{in}}}^{T_c(z)} c_p(T)\, dT = q' \cdot z \tag{4-12}$$

Combining Equations (4-11) and (4-12) gives:

$$\dot{m} \int_{T_{\text{in}}}^{T_c(z)} (150 - 0.01\,T)\, dT = q' \cdot z \tag{4-13}$$

which simplifies to:

$$\dot{m} \left(150\,T - \frac{0.01}{2} T^2\right)\Big|_{T_{in}}^{T_c(z)} = q' \cdot z \tag{4-14}$$

$$-0.005\,T_c^2(z) + 150\,T_c(z) - \left(150\,T_{in} - 0.005\,T_{in}^2 + \frac{q' \cdot z}{\dot{m}}\right) = 0 \qquad (4\text{-}15)$$

The coolant temperature at elevation z can then be found with the quadratic equation:

$$T_c(j) = \frac{-b \pm \sqrt{b^2 - 4ac}}{2a} \qquad (4\text{-}16)$$

where

$$\mathrm{a} = -0.005$$

$$\mathrm{b} = 150$$

$$\mathrm{c} = -1 \times \left[150\,\mathrm{T_{in}} - \frac{0.01}{2}\mathrm{T_{in}^2} + \frac{\mathrm{q'} \cdot \mathrm{z}}{\dot{\mathrm{m}}}\right]$$

The cladding and fuel temperatures can be found by applying the same methodology presented in Sections 3.1.3.2 - 3.1.3.5. Table 4-2 lists the resulting coolant, cladding, and fuel temperatures.

Table 4-2 Variable Heat Capacity Analytical Temperature Solution (K)

Axial Position (m)	Avg. Coolant	Clad Outer	Clad Inner	Fuel Surface	Fuel Centerline
1.02375	797.843	850.965	868.562	1190.614	1596.621
0.97125	792.455	845.578	863.174	1185.226	1591.234
0.91875	787.070	840.192	857.788	1179.841	1585.848
0.86625	781.686	834.809	852.405	1174.457	1580.464
0.81375	776.305	829.427	847.023	1169.075	1575.083
0.76125	770.925	824.048	841.644	1163.696	1569.703
0.70875	765.548	818.670	836.266	1158.318	1564.326
0.65625	760.172	813.295	830.891	1152.943	1558.951
0.60375	754.799	807.921	825.518	1147.570	1553.577
0.55125	749.428	802.550	820.146	1142.198	1548.206
0.49875	744.058	797.181	814.777	1136.829	1542.836
0.44625	738.691	791.813	809.410	1131.462	1537.469
0.39375	733.326	786.448	804.044	1126.096	1532.104
0.34125	727.962	781.085	798.681	1120.733	1526.741
0.28875	722.601	775.724	793.320	1115.372	1521.379
0.23625	717.242	770.364	787.960	1110.013	1516.020
0.18375	711.885	765.007	782.603	1104.655	1510.663
0.13125	706.529	759.652	777.248	1099.300	1505.308
0.07875	701.176	754.299	771.895	1093.947	1499.954
0.02625	695.825	748.947	766.543	1088.596	1494.603

4.2.4 Results Summary

All QOIs are within their respective acceptance criteria. A summary of the results is provided in Table 4-3. The difference between the simulation and the analytical solution is provided in Table 4-4. The SAS4A/SASSYS-1 axial temperature profile agrees very well with the analytical solution for the LFR fuel channel case with temperature dependent heat capacity.

Table 4-3 Summary of Results for Variable Coolant Heat Capacity Case

QOI	Result	Notes
Coolant Temperature	Pass	
Cladding Outer Surface Temperature	Pass	
Cladding Inner Surface Temperature	Pass	
Fuel Surface Temperature	Pass	
Fuel Centerline Temperature	Pass	

Table 4-4 Variable Coolant Heat Capacity Case: Axial Temperature Errors (K)

Axial Position (m)	Avg. Coolant	Clad Outer	Clad Inner	Fuel Surface	Fuel Centerline
1.024	0.000	-0.001	0.013	0.013	0.012
0.971	-0.001	-0.000	0.012	0.012	0.013
0.919	-0.000	-0.001	0.012	0.013	0.012
0.866	0.000	-0.000	0.012	0.012	0.012
0.814	-0.000	0.000	0.012	0.012	0.012
0.761	0.000	-0.000	0.012	0.012	0.012
0.709	-0.000	0.000	0.012	0.012	0.012
0.656	-0.001	-0.000	0.012	0.012	0.013
0.604	-0.000	-0.001	0.013	0.013	0.012
0.551	-0.000	0.000	0.012	0.012	0.012
0.499	0.000	-0.000	0.012	0.012	0.012
0.446	-0.000	-0.001	0.013	0.013	0.012
0.394	-0.000	0.000	0.012	0.012	0.012
0.341	-0.001	-0.000	0.012	0.012	0.013
0.289	0.000	-0.000	0.013	0.012	0.012
0.236	-0.000	-0.001	0.012	0.013	0.012
0.184	-0.000	0.000	0.012	0.012	0.012
0.131	-0.001	-0.000	0.012	0.012	0.013
0.079	0.000	-0.000	0.013	0.012	0.012
0.026	-0.000	-0.001	0.012	0.013	0.012

4.3 Coolant Thermal Conductivity

4.3.1 Test Description

For this case, the thermal conductivity of the coolant is updated from a constant value to:

$$k_c(T) = 9.2 + 0.011 \times T \tag{4-17}$$

where the temperature is in Kelvin and k_c is in $\frac{W}{m-K}$.

4.3.2 Acceptance Criteria

The test case is considered acceptable if there is reasonable agreement between SAS4A/SASSYS-1 results and the analytical solution for the following QOI:

- Fuel centerline temperature,
- Fuel surface temperature,
- Cladding inner surface temperature,
- Cladding outer surface temperature.

All temperature QOIs must be within 0.1 K of the analytic solution.

4.3.3 Analytic Solution

For single-phase liquid metal coolant the convective heat transfer coefficient, h_c, is commonly defined using the Seban-Shimazaki correlation:

$$h_c = \frac{k_c}{D_h}\left(0.025\left[\frac{D_h\,\dot{m}\,c_p}{k_c\,A_c}\right]^{0.8} + 5.0\right) \tag{4-18}$$

where D_h is the hydraulic diameter, k_c is the coolant thermal conductivity, $\dot{m}$ is the mass flow rate, c_p is the coolant specific heat, and A_c is the coolant flow area. Due to the variable nature of the coolant thermal conductivity and the heat capacity, the heat transfer coefficient becomes temperature dependent.

$$h_c\big(T_c(z)\big) = \frac{k_c\big(T_c(z)\big)}{D_h}\left(0.025\left[\frac{D_h\,\dot{m}\,c_p\big(T_c(z)\big)}{k_c\big(T_c(z)\big)A_c}\right]^{0.8} + 5.0\right) \tag{4-19}$$

Using the bulk coolant temperature that was derived in Section 4.2, the cladding outer surface temperature was using in Equation (3-5) as:

$$T_{co}(z) = T_c(z) + \frac{\mathrm{q}'}{2\,\pi\,\mathrm{R_{co}}\,h_c\big(T_c(z)\big)} \tag{4-20}$$

The cladding inner surface and fuel temperatures can be found by applying the same methodology presented in Sections 3.1.3.3 - 3.1.3.5. Table 4-5 lists the resulting coolant, cladding, and fuel temperatures.

Table 4-5 Variable Coolant Thermal Conductivity Case: Analytical Temperature Solution (K)

Axial Position (m)	Avg. Coolant	Clad Outer	Clad Inner	Fuel Surface	Fuel Centerline
1.02375	797.843	815.320	832.916	1154.968	1560.976
0.97125	792.455	809.962	827.558	1149.610	1555.618
0.91875	787.070	804.607	822.203	1144.255	1550.262
0.86625	781.686	799.253	816.849	1138.901	1544.909
0.81375	776.305	793.902	811.498	1133.550	1539.558
0.76125	770.925	788.553	806.149	1128.201	1534.209
0.70875	765.548	783.206	800.802	1122.854	1528.862
0.65625	760.172	777.861	795.457	1117.509	1523.517
0.60375	754.799	772.518	790.114	1112.166	1518.174
0.55125	749.428	767.178	784.774	1106.826	1512.833
0.49875	744.058	761.839	779.435	1101.488	1507.495
0.44625	738.691	756.503	774.099	1096.151	1502.159
0.39375	733.326	751.169	768.765	1090.817	1496.825
0.34125	727.962	745.837	763.433	1085.485	1491.493
0.28875	722.601	740.507	758.103	1080.155	1486.163
0.23625	717.242	735.179	752.775	1074.828	1480.835
0.18375	711.885	729.854	747.450	1069.502	1475.509
0.13125	706.529	724.530	742.126	1064.178	1470.186
0.07875	701.176	719.209	736.805	1058.857	1464.865
0.02625	695.825	713.890	731.486	1053.538	1459.545

4.3.4 Results Summary

All QOIs are within their respective acceptance criteria. A summary of the results is provided in Table 4-6. The difference between the simulation and the analytical solution is provided in Table 4-7. The SAS4A/SASSYS-1 axial temperature profile agrees very well with the analytical solution for the LFR fuel channel case with temperature dependent heat capacity and thermal conductivity.

Table 4-6 Summary of Results for Variable Coolant Thermal Conductivity Case

QOI	Result	Notes
Cladding Outer Surface Temperature	Pass	
Cladding Inner Surface Temperature	Pass	
Fuel Surface Temperature	Pass	
Fuel Centerline Temperature	Pass	

Table 4-7 Variable Coolant Thermal Conductivity Case: Axial Temperature Errors (K)

Axial Position (m)	Avg. Coolant	Clad Outer	Clad Inner	Fuel Surface	Fuel Centerline
1.024	0.000	-0.003	0.009	0.009	0.009
0.971	-0.001	-0.004	0.009	0.009	0.009
0.919	-0.000	-0.003	0.009	0.009	0.009
0.866	0.000	-0.004	0.009	0.009	0.009
0.814	-0.000	-0.003	0.009	0.009	0.009
0.761	0.000	-0.003	0.009	0.009	0.010
0.709	-0.000	-0.003	0.009	0.009	0.010
0.656	-0.001	-0.003	0.009	0.009	0.009
0.604	-0.000	-0.004	0.009	0.009	0.009
0.551	-0.000	-0.003	0.009	0.009	0.009
0.499	0.000	-0.004	0.009	0.010	0.009
0.446	-0.000	-0.003	0.009	0.009	0.009
0.394	-0.000	-0.003	0.009	0.009	0.009
0.341	-0.001	-0.003	0.009	0.009	0.009
0.289	0.000	-0.004	0.009	0.009	0.009
0.236	-0.000	-0.004	0.009	0.009	0.009
0.184	-0.000	-0.003	0.009	0.009	0.009
0.131	-0.001	-0.004	0.009	0.008	0.009
0.079	0.000	-0.003	0.009	0.009	0.009
0.026	-0.000	-0.003	0.009	0.009	0.008

4.4 Built-in Pb Coolant Properties

4.4.1 Test Description

For this case, the coolant density, heat capacity and thermal conductivity will use the built-in correlations for Lead Coolant. The correlation for coolant density is:

$$\rho(T) = A_{12} + A_{13}T + A_{14}T^2 \tag{4-21}$$

where the default values for A_n and T_C are provided in Table 4-8.

The correlation for coolant heat capacity is:

$$c_{\mathrm{p}}(T) = \frac{A_{28}}{(T_c - T)^2} + \frac{A_{29}}{T_c - T} + A_{30} + A_{31}(T_C - T) + A_{32}(T_C - T)^2 \tag{4-22}$$

where the default values for A_n and T_C are provided in Table 4-8.

The correlation for coolant thermal conductivity is:

$$k(T) = A_{48} + A_{49}\,T + A_{50}T^2 + A_{51}T^3 \tag{4-23}$$

where the default values for A_n are provided in Table 4-8.

Table 4-8 Default Values for Correlation Coefficients for Lead

A_n	Value
A_{12}	11441
A_{13}	-1.2795
A_{14}	0.0
A_{28}	1.0
A_{29}	0.0
A_{30}	2.454E+02
A_{31}	-6.672E-02
A_{32}	1.015E-05
A_{48}	9.20
A_{49}	1.10E-02
A_{50}	0.0
A_{51}	0.0
T_C	5.0E3

4.4.2 Acceptance Criteria

The test case is considered acceptable if there is reasonable agreement between SAS4A/SASSYS-1 results and the analytical solution for the following QOI:

- Fuel centerline temperature,

- Fuel surface temperature,
- Cladding inner surface temperature,
- Cladding outer surface temperature,
- Coolant Temperature, and
- Pressure difference between the inlet and outlet of the coolant channel.

All temperature QOIs must be within 0.1 K of the analytic solution. All pressure QOIs must be within 0.1 kPa.

4.4.3 Analytic Solution

Because the above correlations are higher order polynomials, an analytical temperature solution would be very lengthy. Instead, numerical methods for integration and optimization were used to determine the coolant and cladding temperatures. The coolant axial pressure is found by solving Equations (4-2), (4-5), (4-9), and (4-10) with the quad function from scipy. The coolant axial temperature profile is found by solving Equation (4-12) using the quad and root finder functions from scipy. With the coolant temperature known, the cladding outer surface temperature can be found using Equation (4-20). The cladding inner surface temperatures and fuel temperature are found as described in in Sections 3.1.3.3 - 3.1.3.5. Table 4-9 lists the resulting coolant, cladding, and fuel temperatures. The analytical pressure drop between the inlet and outlet of the core channel was found to be 125131.9 Pa.

Table 4-9 Built-In Pb Material Case: Analytical Temperature Solution (K)

Axial Position (m)	Avg. Coolant	Clad Outer	Clad Inner	Fuel Surface	Fuel Centerline
1.02375	795.894	813.265	830.861	1152.913	1558.921
0.97125	790.591	807.988	825.584	1147.637	1553.644
0.91875	785.291	802.716	820.312	1142.364	1548.371
0.86625	779.995	797.446	815.042	1137.095	1543.102
0.81375	774.703	792.181	809.777	1131.829	1537.837
0.76125	769.414	786.919	804.515	1126.567	1532.575
0.70875	764.129	781.661	799.257	1121.310	1527.317
0.65625	758.848	776.407	794.003	1116.055	1522.063
0.60375	753.570	771.157	788.753	1110.805	1516.813
0.55125	748.297	765.910	783.506	1105.558	1511.566
0.49875	743.027	760.667	778.263	1100.316	1506.323
0.44625	737.760	755.428	773.025	1095.077	1501.084
0.39375	732.498	750.193	767.789	1089.842	1495.849
0.34125	727.239	744.962	762.558	1084.610	1490.618
0.28875	721.984	739.735	757.331	1079.383	1485.390
0.23625	716.733	734.511	752.107	1074.159	1480.167
0.18375	711.485	729.291	746.887	1068.940	1474.947
0.13125	706.242	724.075	741.672	1063.724	1469.731
0.07875	701.002	718.864	736.460	1058.512	1464.519
0.02625	695.766	713.656	731.252	1053.304	1459.311

4.4.4 Results Summary

All QOIs are within their respective acceptance criteria. A summary of the results is provided in Table 4-10. The difference between the simulation and the analytical solution is provided in Table 4-11. The error in the channel pressure drop was found to be 0.032 kPa, less than the accuracy of the SAS4A/SASSYS-1 printout. The SAS4A/SASSYS-1 axial temperature profile and channel pressure drop agrees very well with the analytical solution for the LFR fuel channel case with the default Pb temperature dependent material properties.

Table 4-10 Summary of Results for Built-In Pb Material Case

QOI	Result	Notes
Coolant Temperature	Pass	
Cladding Outer Surface Temperature	Pass	
Cladding Inner Surface Temperature	Pass	
Fuel Surface Temperature	Pass	
Fuel Centerline Temperature	Pass	
Channel Pressure Drop	Pass	

Table 4-11 Built-In Pb Material Case: Axial Temperature Errors (K)

Axial Position (m)	Avg. Coolant	Clad Outer	Clad Inner	Fuel Surface	Fuel Centerline
1.024	0.000	-0.003	0.009	0.009	0.009
0.971	-0.001	-0.004	0.009	0.009	0.009
0.919	-0.000	-0.003	0.009	0.009	0.009
0.866	0.000	-0.004	0.009	0.009	0.009
0.814	-0.000	-0.003	0.009	0.009	0.009
0.761	0.000	-0.003	0.009	0.009	0.010
0.709	-0.000	-0.003	0.009	0.009	0.010
0.656	-0.001	-0.003	0.009	0.009	0.009
0.604	-0.000	-0.004	0.009	0.009	0.009
0.551	-0.000	-0.003	0.009	0.009	0.009
0.499	0.000	-0.004	0.009	0.010	0.009
0.446	-0.000	-0.003	0.009	0.009	0.009
0.394	-0.000	-0.003	0.009	0.009	0.009
0.341	-0.001	-0.003	0.009	0.009	0.009
0.289	0.000	-0.004	0.009	0.009	0.009
0.236	-0.000	-0.004	0.009	0.009	0.009
0.184	-0.000	-0.003	0.009	0.009	0.009
0.131	-0.001	-0.004	0.009	0.008	0.009
0.079	0.000	-0.003	0.009	0.009	0.009
0.026	-0.000	-0.003	0.009	0.009	0.008

5 Primary Heat Transport System Cases

In previous sections, SAS4A/SASSYS-1 has used boundary conditions at the inlet and outlet of the core channel. The core inlet temperature and mass flow rate have been supplied as input. A specified core outlet pressure has served as a reference pressure for determining the channel axial pressure. The following cases test various aspects of the PRIMAR-4 module, which simulates the thermal hydraulic behavior of the heat removal systems in SAS4A/SASSYS-1, removing the need for predetermined boundary conditions at the core inlet and outlet.

5.1 Equilibrium PRIMAR-4 Temperatures

5.1.1 Test Description

The equilibrium PRIMAR-4 temperature test case is designed to test the ability of SAS4A/SASSYS-1 to model the distribution of temperatures throughout the primary heat transport loop. The primary loop layout, shown in Figure 5-1, is based on the layout of the CIRCE-ICE experimental campaign [12]. The core channel is an extension of the LFR fuel channel geometry summarized in Table 3-1. The number of fuel rods has been increased to match the CIRCE-ICE specifications. The reactor power and flow rate have been scaled by the number of pins, preserving the temperature rise across the core. A gas plenum, upper reflector and lower reflector have been included in the core channel, extending the core channel height to 2.367 m. After entering the core channel from the inlet plenum, CV1, lead travels upwards until it reaches the outlet plenum, CV2. From the outlet plenum the lead travels through the coolant pump until it reaches the hot pool, CV3. After exiting the hot pool, the lead travels through the primary heat exchanger and enters the cold pool, CV4. From the cold pool the lead passes through a small piping network and enters the inlet plenum. Segment 2 contains the reactor coolant pump, E3, and two connected pipes, E2 and E4. E2 contains 1 bend. The shell side of the primary heat exchanger is E5, which belongs to segment 3. The tube side of the primary heat exchanger is E7, which does not belong to a segment but has temperature and mass flow rate boundary conditions applied at the inlet. Segment 4 is an artificial pipe, E6, connecting the inlet plenum to the cold pool. A summary of the primary loop geometry is provided in Table 5-1, Table 5-2, and Table 5-3.

This test case can be broken into three subtests. The first subtest will confirm that SAS4A/SASSYS-1 correctly distributes the core inlet temperature and core outlet temperature throughout the system. In addition to distributing the temperature throughout the system the temperature profile in the detailed primary heat exchanger must be calculated correctly. In the second subtest a zero transient will be performed to ensure SAS4A/SASSYS-1 maintains the steady state conditions. In the third subtest, the inlet to the secondary side of the primary heat exchanger will be increased by 10 K over 100 seconds followed by an additional 29,800 seconds of simulation time to allow the system to come to a new equilibrium. The third subtest will confirm that SAS4A/SASSYS-1 correctly reaches a new equilibrium temperature distribution.

5.1.2 Acceptance Criteria

The test case is considered acceptable if there is reasonable agreement between SAS4A/SASSYS-1 results and the analytical solution for the following QOI:

- Temperature between the inlet of the primary heat exchanger and the core outlet,

- Temperature between the outlet of the primary heat exchanger and core inlet,
- Temperature profile within the primary heat exchanger.

All temperature QOIs must be within 0.1 K.

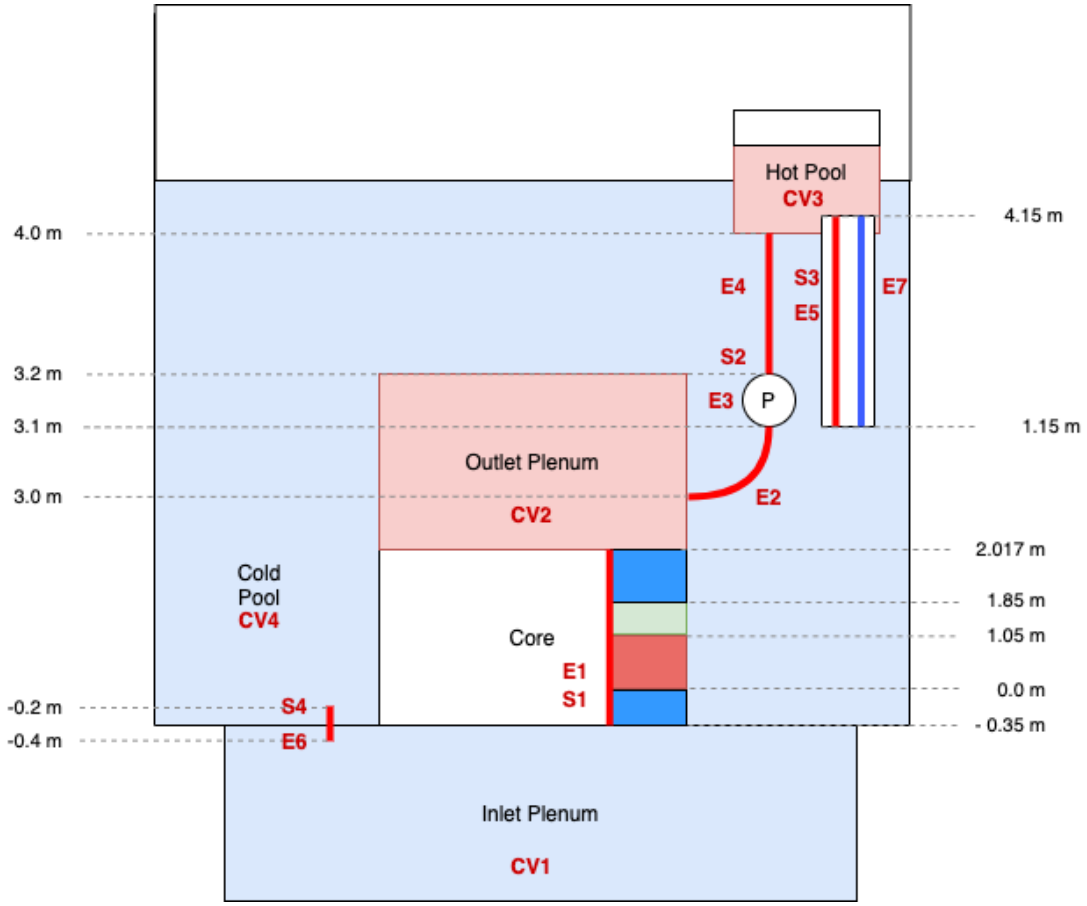

Figure 5-1 Primary Loop Layout for the LFR Primary System Cases

Table 5-1. Core Channel Parameters for the LFR Primary System Cases

Core Channel		
# Pins	-	37
Coolant Inlet Temp	K	693.15
Core Outlet Pressure	Pa	6.6143E+05
Mass Flow Rate Per Pin	kg/s	0.98
Total Power	kW	555
Number of Lower Reflector Nodes	-	1
Number of Fuel Nodes	-	20
Number of Plenum Nodes	-	1
Number of Upper Reflector Nodes	-	1
Number of Radial Fuel Nodes	-	9
Pin Dimensions		
Lower Reflector Height	m	0.35
Fuel Height	m	1.05
Gas Plenum Height	m	0.8
Upper Reflector Height	m	0.167
Fuel Radius	m	4.275E-03
Cladding Inner Radius	m	4.450E-03
Cladding Outer Radius	m	5.350E-03
Reflector Inner Thickness	m	2.675E-3
Reflector Outer Thickness	m	2.675E-3
Inner Structure Thickness	m	1.0E-08
Outer Structure Thickness	m	1.0E-08
Inner Structure Perimeter	m	1.0E-08
Hydraulic Diameter	m	8.044E-03
Coolant Flow Area Per Pin	m^2	6.760E-05
Wetted Perimeter	m	3.362E-02
Thermo-Physical Properties		
Fuel Thermal Conductivity	W/m-K	2.8
Cladding Thermal Conductivity	W/m-K	23.8
Gap Thermal Conductivity	W/m-K	0.289
Other Values		
Channel Friction Factor Correlation Coefficients	[AFR, BFR]	[0.316, -0.25]
Channel Film Heat Transfer Coef. Correlation Coefficients	[C1, C2, C3]	[0.0281, 0.77, 7.030]

Table 5-2. System Parameters for the LFR Primary System Cases

Element	Inlet Elevation	Outlet Elevation	Length	Area	Hydraulic Diameter
[-]	[m]	[m]	[m]	[m^2]	[m]
1	-0.35	2.017	2.367	1.0	1.0
2	3.0	3.1	0.2	0.0324	0.202
3	3.1	3.2	0.1	0.0323	0.203
4	3.2	4.0	0.8	0.0322	0.204
5	4.15	1.15	3.0	0.0459	0.021
6	-0.4	-0.2	0.2	1.075	1.170
7	1.15	4.15	3.0	0.0321	0.02118

Element	Surface Roughness	Orifice Coefficient	Number of Bends	Pipe Wall Heat Capacity per Length	Pipe Wall Heat Transfer Coef.
[-]	[m]	[-]	[-]	[J/K-m]	[W/m^2-K]
1	1.0	0.0	0.0	1.0	1.0
2	7.0E-06	0.0	1.0	7.71770E+04	5.68800E+03
3	8.0E-06	0.0	0.0	7.71770E+04	5.68800E+03
4	9.0E-06	0.0	0.0	7.71770E+04	5.68800E+03
5	1.0E-05	0.5	0.0	7.71770E+04	5.68800E+03
6	2.0E-05	0.0	0.0	7.71770E+04	5.68800E+03
7	3.0E-05	0.0	0.0	7.71770E+04	5.68800E+03

Compressible Volume	Total Volume	Initial Gas Volume	Initial Gas Pressure	Liquid-Gas Surface Area	Reference Height
[-]	[m^3]	[m^3]	[Pa]	[m^2]	[m]
1	0.86	0.0	-	-	-0.35
2	0.14	0.0	-	-	2.017
3	0.2	0.1	286979	0.2	4.0
4	5.5	0.3	286979	0.4	4.0

Compressible Volume	Coolant Thermal Expansion	Volume Thermal Expansion	Wall Area	Wall Heat Capacity	Wall Heat Transfer Coef.
[-]	[1/K]	[1/K]	[m^2]	[J/K]	[W/m^2-K]
1	-1.13715E-04	2.0E-05	1.0	1.0E6	520
2	-1.13715E-04	2.0E-05	2.0	1.0E6	2600
3	-1.13715E-04	2.0E-05	0.2	1.0E6	2600
4	-1.13715E-04	2.0E-05	7.0	1.0E6	520

Table 5-3. Heat Exchanger Parameters for the LFR Primary System Cases

Heat Exchanger Properties		
Number of Tubes	-	91
Number of Axial Nodes	-	20
Tube ID	m	0.02118
Tube OD	m	0.0254
Shell ID	m	0.3423
Shell OD	m	0.3623
Tube Thermal Conductivity	W/m-K	13
Shell Thermal Conductivity	W/m-K	13
Tube Volumetric Heat Capacity	J/K-m^3	4.0E6
Shell Volumetric Heat Capacity	J/K-m^3	4.0E6
Shell Coolant	-	Pb
Tube Coolant	-	PbBi
Shell HTC Correlation Coefficients	[C1, C2, C3, C4]	[0.018, 0.8, 4.5, 0.0]
Tube HTC Correlation Coefficients	[C1, C2, C3, C4]	[0.023, 0.8, 0.0, -0.4]

5.1.3 Analytical Solution

5.1.3.1 Hot Leg Temperature

Adiabatic boundary conditions will be applied on the pipe walls between the outlet of the core channel to the inlet of the heat exchanger. Therefore, all components between the core channel outlet and the primary heat exchanger inlet should be at the exit temperature of the core channel. A derivation for the core channel outlet temperature has been provided in Section 4.4.3. At the end of the steady state calculation and the zero transient, the hot leg temperature should be 798.54 K. At the end of the transient calculation, the hot leg temperature should be 808.60 K.

5.1.3.2 Primary Heat Exchanger Temperature

The primary heat exchanger model utilizes the detailed shell-tube heat exchanger model within SAS4A/SASSYS-1. The detailed shell-tube heat exchanger model is composed of four axial components, the shell wall, shell coolant, tube wall and tube coolant. Assuming axial conduction is negligible in the shell wall, the shell axial temperature distribution is governed by:

$$\left(\rho c_p\right)_s P_{s-sc}\, d_s \frac{\partial T_s}{\partial t} = P_{s-sc}\, H_{s-sc}\, (T_{sc} - T_s) + (hA)_{snk}\, (T_{snk} - T_s) \tag{5-1}$$

where $\left(\rho c_p\right)_s$ is the shell wall heat capacity per unit volume, P_{s-sc} is the perimeter between the shell wall and the shell coolant, d_s is the thickness of the shell, T_s is the temperature of the shell wall, H_{s-sc} is the heat transfer coefficient between the shell wall and the shell coolant, T_{sc} is the shell coolant temperature, $(hA)_{snk}$ is the heat transfer coefficient times surface area per unit length between the shell wall and an external heat sink, and T_{snk} is the temperature of an external heat sink. H_{s-sc} is defined as:

$$H_{s-sc} = \left(\frac{1}{h_{sc}} + \frac{d_s}{2 \cdot k_s} + \frac{1}{h_{Fs}}\right)^{-1} \tag{5-2}$$

where h_{sc} is the film heat transfer coefficient of the shell coolant, k_s is the thermal conductivity of the shell wall and $\frac{1}{h_{Fs}}$ is the shell-side coolant fouling factor, which is assumed to be negligible. h_{sc} is defined as:

$$h_{sc} = \frac{k}{D_h}\left(C_{1,sc} * \left(\frac{D_h|\dot{m}|}{A\mu}\right)^{C_{2,sc}} \left(\frac{c_p\mu}{k}\right)^{C_{4,sc}} + C_{3,sc}\right) \tag{5-3}$$

where k is the thermal conductivity, $D_h$is the hydraulic diameter, A is the cross-sectional flow area, $\dot{m}$ is the mass flow rate of the shell, μ is the fluid viscosity, c_p is the fluid specific heat capacity and $C_{1,sc} - C_{4,sc}$ are user-defined coefficients. All fluid properties are defined at the bulk shell coolant temperature and D_h and A are parameters of the shell coolant. Under the assumption that an external heat sink is not present and steady state conditions, the shell wall temperature simplifies to

$$T_s = T_{sc} \tag{5-4}$$

The shell coolant axial temperature distribution is governed by:

$$A_{sc}\,\rho_{sc}c_{p_{sc}}\frac{\partial T_{sc}}{\partial t} + w_s c_{p_{sc}}\frac{\partial T_{sc}}{\partial z} = P_{s-sc}\,H_{s-sc}\,(T_s - T_{sc}) + P_{t-sc}\,H_{t-sc}\,S\,(T_t - T_{sc}) \tag{5-5}$$

where A_{sc} is the shell cross-sectional flow area, ρ_{sc} is the density of the shell coolant, $c_{p_{sc}}$ is the specific heat capacity of the shell coolant, w_s is the shell coolant flow rate, S is the tube slant factor, P_{t-sc} is the perimeter between the tube wall and the shell coolant, T_t is the tube temperature, and H_{t-sc} is the heat transfer coefficient between the tube wall and the shell coolant. H_{t-sc} is defined as:

$$H_{s-sc} = \left(\frac{1}{h_{sc}} + \frac{d_t}{2 \cdot k_t} + \frac{1}{h_{Fs}}\right)^{-1} \tag{5-6}$$

where d_t is the thickness of the tube, and k_t is the thermal conductivity of the tube wall. Under steady state conditions and a slant factor of 1, the shell coolant temperature simplifies to:

$$w_s c_{p_{sc}}\frac{\partial T_{sc}}{\partial z} = P_{t-sc}\,H_{t-sc}(T_t - T_{sc}) \tag{5-7}$$

Assuming axial conduction is negligible in the tube wall, the tube axial temperature distribution is governed by:

$$\left(\rho c_p\right)_t 0.5(P_{t-sc} + P_{t-tc}) S\, d_t \frac{\partial T_t}{\partial t} = P_{s-sc}\, H_{t-sc}\, S\, (T_{sc} - T_t) + P_{t-tc}\, H_{t-tc}\, S(T_{tc} - T_t) \tag{5-8}$$

where $\left(\rho c_p\right)_t$ is the tube wall heat capacity per unit volume, P_{t-tc} is the perimeter between the tube wall and the tube coolant, T_{tc} is the temperature of the tube coolant, H_{t-tc} is the heat transfer coefficient between the tube wall and the tube coolant, defined as:

$$H_{t-tc} = \left(\frac{1}{h_{tc}} + \frac{d_t}{2 \cdot k_t} + \frac{1}{h_{Ft}}\right)^{-1} \tag{5-9}$$

where h_{tc} is the film heat transfer coefficient of the tube coolant, and $\frac{1}{h_{Ft}}$ is the tube-side coolant fouling factor, which is assumed to be negligible. h_{tc} is defined as:

$$h_{tc} = \frac{k}{D_h}\left(C_{1,tc} * \left(\frac{D_h|\dot{m}|}{A\mu}\right)^{C_{2,tc}} \left(\frac{c_p \mu}{k}\right)^{C_{4,tc}} + C_{3,tc}\right) \tag{5-10}$$

where k is the thermal conductivity, $D_h$is the hydraulic diameter, A is the cross-sectional flow area, $\dot{m}$ is the mass flow rate of the tube, μ is the fluid viscosity, c_p is the fluid specific heat capacity and $C_{1,tc} - C_{4,tc}$ are user-defined coefficients. All fluid properties are defined at the bulk tube coolant temperature and D_h and A are parameters of the tube. Under the assumption of steady state conditions and a uniform slant factor, the tube wall temperature simplifies to

$$T_t = \frac{(P_{s-sc}\, H_{t-sc}\, T_{sc} + P_{t-tc}\, H_{t-tc}\, T_{tc})}{P_{s-sc}\, H_{t-sc} + P_{t-tc}\, H_{t-tc}} \tag{5-11}$$

The tube coolant axial temperature distribution is governed by:

$$A_{tc}\, \rho_{tc} c_{p_{tc}} \frac{\partial T_{tc}}{\partial t} + w_t c_{p_{tc}} \frac{\partial T_{tc}}{\partial z} = P_{t-sc}\, H_{t-sc}\, S\, (T_t - T_{tc}) \tag{5-12}$$

where A_{tc} is the tube cross-sectional flow area, ρ_{tc} is the density of the tube coolant, $c_{p_{tc}}$ is the specific heat capacity of the tube coolant, w_t is the tube coolant flow rate. Under the assumption of steady state conditions, and uniform slant factor, this simplifies to:

$$w_t c_{p_{tc}} \frac{\partial T_{tc}}{\partial z} = P_{t-sc}\, H_{t-sc}\, S\, (T_t - T_{tc}) \tag{5-13}$$

Equations (5-7) and (5-13) are coupled partial differential equations. Together with Equations (5-6), (5-9), and (5-11) the system of partial differential equations can be solved using numeric techniques. The boundary conditions for the coupled differential equations vary depending on what is being investigated. During steady state initialization, both boundary conditions will be applied on the primary coolant, as the inlet and outlet of the primary heat exchanger are already known. At the end of the transient, the boundary conditions are applied on the secondary side of the heat exchanger, assuming the heat exchanger is balancing the heat being produced by the reactor core. The temperature solution for the shell and tube coolant at the end of the steady state and transient calculation are presented in Table 5-4.

Table 5-4. Heat Exchanger Temperature Distribution (K)

	Steady State		End of Transient	
Axial Position (m)	**Shell Coolant**	**Tube Coolant**	**Shell Coolant**	**Tube Coolant**
3.000	798.547	791.637	808.598	801.778
2.850	794.010	786.981	804.110	797.164
2.700	789.401	782.251	799.545	792.473
2.550	784.720	777.446	794.904	787.702
2.400	779.965	772.566	790.185	782.852
2.250	775.136	767.610	785.387	777.920
2.100	770.231	762.576	780.509	772.906
1.950	765.250	757.464	775.549	767.808
1.800	760.192	752.272	770.508	762.626
1.650	755.056	747.000	765.383	757.358
1.500	749.841	741.647	760.175	752.004
1.350	744.546	736.213	754.881	746.562
1.200	739.170	730.695	749.500	741.031
1.050	733.712	725.093	744.032	735.410
0.900	728.172	719.406	738.476	729.698
0.750	722.549	713.634	732.830	723.894
0.600	716.841	707.775	727.093	717.997
0.450	711.048	701.829	721.265	712.006
0.300	705.169	695.794	715.345	705.920
0.150	699.203	689.671	709.331	699.737
0.000	693.150	683.457	703.222	693.457

5.1.3.1 Cold Leg Temperature

Adiabatic boundary conditions will be applied on the pipe walls between the outlet of the heat exchanger to the inlet of the core channel. Therefore, all components between the heat exchanger outlet and the core channel inlet should be at the exit temperature of the heat exchanger. A derivation for the heat exchanger outlet temperature has been provided in Section

5.1.3.2. At the end of the steady state calculation and the zero transient, the cold leg temperature should be 693.15 K. At the end of the transient calculation, the cold leg temperature should be 703.22.

5.1.4 Results Summary

All QOIs are within their respective acceptance criteria. A summary of the results is provided in Table 5-5. The difference between the simulation and the analytical solution is provided in Table 5-6. The maximum error in the heat exchanger temperature distribution was found to be 0.0002 K, less than the accuracy of the SAS4A/SASSYS-1 printout. Similar to the heat exchanger distribution, the SAS4A/SASSYS-1 hot and cold leg temperatures profile agree very well with the analytical solution.

Table 5-5. Summary of Results for PRIMAR-4 Temperature Case

QOI	Result	Notes
Steady State Hot Leg Temperature	Pass	
Steady State Cold Leg Temperature	Pass	
Steady State Shell Coolant Temperature	Pass	
Steady State Tube Coolant Temperature	Pass	
Transient Hot Leg Temperature	Pass	
Transient Cold Leg Temperature	Pass	
Transient Shell Coolant Temperature	Pass	
Transient Tube Coolant Temperature	Pass	

Table 5-6. Heat Exchanger Temperature Axial Error.

	Steady State		End of Transient	
Axial Position (m)	**Shell Coolant**	**Tube Coolant**	**Shell Coolant**	**Tube Coolant**
3.000	0.000	-0.000	0.000	-0.000
2.850	0.000	-0.000	0.000	-0.000
2.700	0.000	-0.000	0.000	-0.000
2.550	0.000	-0.000	0.000	-0.000
2.400	0.000	-0.000	0.000	-0.000
2.250	0.000	-0.000	0.000	-0.000
2.100	0.000	-0.000	0.000	-0.000
1.950	0.000	-0.000	0.000	-0.000
1.800	0.000	-0.000	0.000	-0.000
1.650	0.000	-0.000	0.000	-0.000
1.500	0.000	-0.000	0.000	-0.000
1.350	0.000	-0.000	0.000	-0.000
1.200	0.000	-0.000	0.000	-0.000
1.050	0.000	-0.000	0.000	-0.000
0.900	0.000	-0.000	0.000	-0.000
0.750	0.000	-0.000	0.000	-0.000
0.600	0.000	-0.000	0.000	-0.000
0.450	0.000	-0.000	0.000	-0.000
0.300	0.000	-0.000	0.000	-0.000
0.150	0.000	-0.000	0.000	-0.000
0.000	0.000	-0.000	0.000	-0.000

5.2 Equilibrium PRIMAR-4 Pressures

5.2.1 Test Description

The equilibrium PRIMAR-4 pressure test case is designed to test the ability of SAS4A/SASSYS-1 to model the distribution of pressure throughout the primary heat transport loop. The SAS4A/SASSYS-1 input utilized for the equilibrium PRIMAR-4 temperature test case is also used for the equilibrium PRIMAR-4 pressure test case. This test case can be broken into three subtests. The first subtest will confirm that SAS4A/SASSYS-1 correctly distributes the pressure throughout the system. In addition to distributing the pressure throughout the system, the steady state pressure head must be calculated correctly. In the second subtest a zero transient is performed to ensure SAS4A/SASSYS-1 maintains the steady state conditions. In the third subtest, the inlet to the secondary side of the primary heat exchanger is increased by 10 K over 100 seconds followed by an additional 29800 seconds of simulation time to allow the system to come to a new equilibrium. The third subtest will confirm that SAS4A/SASSYS-1 correctly reaches a new equilibrium pressure distribution, given the new equilibrium temperature distribution. The temperature distributions in each of the segments and CVs is presented in Table 5-7.

Table 5-7. Primary System Steady State Temperature Distribution

	Temperature (K)	
Component	**Steady State Initialization**	**End of Transient**
CV 1	693.15	703.22
CV 2	798.55	808.60
CV 3	798.55	808.60
CV 4	693.15	703.22
Segment 1	See Table 4-9	
Segment 2	798.55	808.60
Segment 3	See Table 5-4	
Segment 4	693.15	703.22

5.2.2 Acceptance Criteria

The test case is considered acceptable if there is reasonable agreement between SAS4A/SASSYS-1 results and the analytical solution for the following QOI:

- Pressure drops in segments two through four,
- Pressure in the compressible volumes,
- Steady state Liquid/Gas interface elevation,
- And Pump Head.

All pressure QOIs must be within 0.1 kPa. distribution.

5.2.3 Analytical Solution

5.2.3.1 Segment Pressure Drop

In addition to friction, gravitation and acceleration pressure drops, PRIMAR-4 accounts for minor pressure losses and pressure losses due to bends. The analytic solution for gravitational and acceleration pressure drop was presented in Sections 4.1.3.1 and 4.1.3.3, respectively. The analytic solution for frictional pressure drop follows the derivation presented in Section 4.1.3.2, however the friction factor is determined using

$$f = \begin{cases} 0.0055\left(1+\left(20000\frac{\epsilon}{D_h}+\frac{1.0E6}{Re}\right)^{\frac{1}{3}}\right), & Re > 1082 \\ \frac{64}{Re}, & Re \leq 1082 \end{cases} \tag{5-14}$$

$$Re = \frac{D_h|w|}{A\mu} \tag{5-15}$$

where D_h is the hydraulic diameter of the element, ϵ is the roughness of the element, w is the element flow rate, A is the element cross sectional area, and μ is the viscosity of the element coolant. The minor pressure loss is described using:

$$\Delta p_K(E) = G\frac{w|w|}{2\rho A^2} \tag{5-16}$$

where G is the orifice coefficient for the element, and ρ is the element coolant density. Currently, SAS4A/SASSYS-1 does not account for directional orifice coefficients, therefore the average density of the element is used for the determination of minor losses. The pressure losses due to bends are described using:

$$\Delta p_B(E) = f\frac{L_B}{D_B}N_B\frac{w|w|}{2\rho A^2} \tag{5-17}$$

where L_B/D_B is an effective length-to-diameter ratio per bend, and N_B is the number of bends within the element. The total pressure drop within an element can then be found using

$$\Delta p(E_i) = p\left(E_{i,in}\right) - p\left(E_{i,out}\right) = \Delta p_{\text{acc.}}\left(E_{i,in,out}\right) + \Delta p_{fric}\left(E_{i,in,out}\right) + \Delta p_{\text{grav}}\left(E_{i,in,out}\right) + \Delta p_K(E_i) + \Delta p_B(E_i) \quad (5\text{-}18)$$

The pressure drop within a segment can then be found by summing the contribution from each element within the segment.

$$\Delta p\left(S_j\right) = \sum_{i \in j} \Delta p(E_i) \quad (5\text{-}19)$$

Table 5-8. Primary System Segment Pressure Drop.

	Pressure Drop (Pa)	
Component	**Steady State Initialization**	**End of Transient**
Segment 2	103143.5	103021.0
Segment 3	-297393.1	-297363.2
Segment 4	-20644.9	-20619.6

5.2.3.2 Compressible Volume Pressure

It is important to note that the pressure drop within the core channel, Segment 1, is not calculated by PRIMAR-4. The coupling of the core channel with the PRIMAR-4 is accomplished through the inlet and outlet plenum pressure and temperature. The core channel inlet and outlet plenum pressures are transferred to their respective PRIMAR-4 compressible volumes. During this transfer, the pressure is adjusted to account for any change in elevation that may exist between the reference CV elevation and the channel inlet and outlet plenum elevation. The pressure for CV2 is found using

$$p(CV_2) = p(Outlet) + g\rho_{CV_2}\left(z_{Outlet} - z_{CV_2}\right) \quad (5\text{-}20)$$

where z_{Outlet} is the reference elevation for the core outlet plenum, z_{CV_2} is the reference elevation for CV2, ρ_{CV_2} is the density of the coolant in CV2, and $P(CV_2)$ is the coolant pressure of CV2, and $P(Outlet)$ is the core channel outlet plenum pressure. Similarly, the pressure in CV1 is

$$p(CV_1) = p(Inlet) + g\rho_{CV_1}\left(z_{Inlet} - z_{CV_1}\right) \quad (5\text{-}21)$$

At steady state, the pressure for CV3 and CV4 is calculated by following the flow path. The steady state pressure for CV 4 is found using

$$p(CV_4) = p(CV_1) + g\rho_{CV_1}\left(z_{CV_1} - z_{S_{4,out}}\right) + g\rho_{CV_4}\left(z_{S_{4,in}} - z_{CV_4}\right) + \Delta P(S_4) \quad (5\text{-}22)$$

where $z_{S_{4,in}}$ and $z_{S_{4,out}}$ are the inlet and outlet elevation of segment 4. Because Segment 2 contains a pump, the steady state pressure of CV3 is found using

$$p(CV_3) = p(CV_4) + g\rho_{CV_4}\left(z_{CV_4} - z_{S_{3,out}}\right) + g\rho_{CV_3}\left(z_{S_{3,in}} - z_{CV_3}\right) + \Delta P(S_3) \quad (5\text{-}23)$$

Given CV3 and CV4 have a common cover gas, the initial elevation of the gas-liquid interface in each pool is calculated using the user provided cover gas pressure, $p(Cg)$.

$$z_{g,CV_i} = z_{CV_i} - \frac{\left(p(Cg) - p(CV_i)\right)}{g\rho_{CV_i}} \quad (5\text{-}24)$$

During steady state initialization, the core inlet and outlet plenum pressure are known, therefore PRIMAR-4 should distribute the pressure along the flow path using Equations (5-20) through (5-24). In order to verify the transient pressure distribution, the cover gas pressure and liquid/gas interface elevation can be used to work backwards to find each of the CV pressures.

Table 5-9. Primary System CV Pressure

CV	Pressure (Pa)		Interface Height (m)	
	Steady State Initialization	End of Transient	Steady State Initialization	End of Transient
1	963081	972135.3	-	-
2	661430	670918.9	-	-
3	526137	535749.6	6.3469	6.3581
4	514054	523631.6	6.1998	6.2104

5.2.3.3 Pump Head

SAS4A/SASSYS-1 will calculate the necessary pump head to achieve the user supplied initial coolant mass flow rate. An analytic value for the pump head, P_H, can be found by comparing the pressure difference between CV2 and CV3.

$$P_H = g\rho_{CV_3}\left(z_{CV_3} - z_{S_{2,out}}\right) - g\rho_{CV_2}\left(z_{S_{2,in}} - z_{CV_2}\right) + \Delta P(S_4) - \left(p(CV_2) - p(CV_3)\right) \quad (5\text{-}25)$$

The steady state pump head, 68,023.7 Pa, should be maintained for entirety of the SAS4A/SASSYS-1 simulation.

5.2.4 Results Summary

All steady state QOIs are within their respective acceptance criteria. Due to a simplification in the transient solver, the error in the pressure distribution at the end of the transient exceeds the acceptance criteria. A summary of the results is provided in Table 5-10. The difference between the simulation and the analytical solution is provided in Table 5-11 and Table 5-12.

Table 5-10. Summary of Results for PRIMAR-4 Pressure Case

QOI	Result	Notes
Steady State Segment Pressure Drops	Pass	
Steady State CV Pressures	Pass	
Steady State CV Interface Height	Pass	
Steady State Pump Head	Pass	
Transient Segment Pressure Drops	Pass	
Transient CV Pressures	Pass	
Transient Pump Head	Pass	

5.2.4.1 Segment Pressure Drops

The difference between the analytical pressure drops and the SAS4A/SASSYS-1 predictions was found to be small. It is observed that the error in the pressure drops increases from the steady state calculation to the transient calculation. This increase is due to an error in the SAS4A/SASSYS-1 temperature referencing during hydraulic calculations. All pressure drops, other than the gravitational pressure drop use the steady state temperatures during the transient calculation. This error is known and is scheduled to be corrected in a subsequent version of SAS4A/SASSYS-1.

Table 5-11. Primary System Segment Pressure Drop Errors.

Component	Pressure Drop (Pa)	
	Steady State Initialization	End of Transient
Segment 2	35.35	35.1
Segment 3	0.79	-9.3
Segment 4	0.0	-0.1

5.2.4.2 Compressible Volume Pressure

The SAS4A/SASSYS-1 predictions and the analytical values for the CV pressures are found to be in excellent agreement. Due to the method selected for calculating the analytical CV pressures at the end of the transient, the error introduced by the segment pressure drops is masked in the CV comparisons. The error would be evident in the liquid/gas elevations.

Table 5-12. Primary System CV Pressure Errors

CV	Pressure (Pa)		Interface Height (m)	
	Steady State Initialization	End of Transient	Steady State Initialization	End of Transient
1	0.02	0.18	-	-
2	0.00	-1.01	-	-
3	0.82	-0.02	1.20E-5	-
4	0.02	0.09	4.17E-6	-

5.2.4.3 Pump Head

The error in the pump head was found to be 36 Pa. Upon further investigation, it was determined that this error is equal to the error in the segment 2 steady state pressure drop. Therefore, it can be concluded that SAS4A/SASSYS-1 is simplifying the reported pump head by subtracting the pressure drop within the pump. This simplification is consistent to what would be measurable in an experiment.

6 Conclusion

Although SAS4A/SASSYS-1 was designed for liquid metal reactors, its historical V & V efforts have focused on sodium fast reactors. In order to support LFR licensing and design studies, an extensive review of the SAS4A/SASSYS-1 test suite was performed. The majority of the V&V test suite was determined to be coolant independent. All reactor power and control system verification problems are independent of the facility layout and the built-in coolant properties. Material property and primary heat transport system verification was determined to have the largest gaps in terms of LFR applicability. To efficiently extend the test suite coverage, seven test cases were created focusing on lead-based systems. Steady-State and Transient test cases were developed in order to demonstrate the initialization routines properly traversed the new LFR layout and the transient routines maintained the correct solution.

Additional work is required to close remaining gaps in the verification testing of SAS4A/SASSYS-1. Future efforts will focus on developing verification tests that are reactor-type agnostic such that the test suite coverage is extended for both SFRs and LFRs. In combination with the ongoing validation efforts, the comprehensive SAS4A/SASSYS-1 verification test suite summarized in this report demonstrates the applicability of SAS4A/SASSYS-1 for LFR design and licensing activities.

Acknowledgement

This work was sponsored by the U.S. Department of Energy's (DOE) Technology Commercialization Fund (TCF), which targets collaborative research between DOE and industry partners. This work has significantly benefited from collaborations and input from Jun Liao, Daniel Wise, and Paolo Ferroni from WEC, and Sung Jin Lee from Fauske and Associates. The submitted manuscript has been created by UChicago Argonne, LLC, Operator of Argonne National Laboratory ("Argonne"). Argonne, a U.S. Department of Energy Office of Science laboratory, is operated under Contract No. DE-AC02-06CH11357.

References

[1] T. H. Fanning, A. J. Brunett, and T. Sumner, eds., "The SAS4A/SASSYS-1 Safety Analysis Code System: User's Guide," Argonne National Laboratory, ANL/NE-16/19, 2017.

[2] A. J. Brunett, L. Ibarra, T. H. Fanning, and R. Hu, "Improvements and Path Forward for Regulatory Acceptance of SAS4A/SASSYS-1," Argonne National Laboratory, ANL/NSE-18/13, 2018.

[3] N. A. A. C. Parisi, F. N. Gleicher, S. Yoon, A. J. Brunett, D. O'Grady, L. Ibarra, and T. Fanning, "Verification and Validation of SAS4A/SASSYS-1 for the Versatile Test Reactor: RVACS," presented at the ANS Virtual Winter Meeting, Online, November 16-19, 2020, 2020.

[4] T. Sumner, T. H. Fanning, and A. J. Brunett, "unpublished information," Argonne National Laboratory, 2014.

[5] T. Fanning, "unpublished information," Argonne National Laboratory 2020.

[6] T. Fanning, "unpublished information," Argonne National Laboratory 2017.

[7] A. Karahan, "unpublished information," Argonne National Laboratory 2020.

[8] D. O'Grady, "unpublished information," Argonne National Laboratory 2020.

[9] T. Sumner, T. H. Fanning, and A. J. Brunett, "unpublished information," Argonne National Laboratory, 2018.

[10] A. J. Brunett, A. Bullerwell, A. J. Dix, and T. Sumner, "unpublished information," Argonne National Laboratory, 2019.

[11] N. E. Todreas and M. S. Kazimi, *Nuclear System I: Thermal Hydraulic Fundamentals*. New York, NY: Taylor & Francis, 1993.

[12] M. Tarantino *et al.*, "Integral Circulation Experiment: Thermal–hydraulic simulator of a heavy liquid metal reactor," *Journal of nuclear materials,* vol. 415, no. 3, pp. 433-448, 2011.

Nuclear Science Engineering Division
Argonne National Laboratory
9700 South Cass Avenue
Argonne, IL 60439

www.anl.gov

Argonne National Laboratory is a U.S. Department of Energy
laboratory managed by UChicago Argonne, LLC